High-resolution angle-resolved photoemission investigation of the quasiparticle scattering processes in a model Fermi liquid: $1T$-$TiTe_2$

L. Perfetti, C. Rojas, A. Reginelli, L. Gavioli,* H. Berger, G. Margaritondo, and M. Grioni
Institut de Physique Appliquée, Ecole Polytechnique Fédérale (EPFL), CH-1015 Lausanne, Switzerland

R. Gaál and L. Forró
Laboratoire de Physique des Solides Semicristallins, IGA, Ecole Polytechnique Fédérale (EPFL), CH-1015 Lausanne, Switzerland

F. Rullier Albenque
Laboratoire des Solides Irradis, CEA-CEREM, Ecole Polytechnique, F-91128 Palaiseau Cedex, France
(Received 8 January 2001; revised manuscript received 9 April 2001; published 22 August 2001)

We present a combined angle-resolved photoemission spectroscopy and resistivity study of the model Fermi liquid system $1T$-$TiTe_2$. From the analysis of the quasiparticle spectral line shape we identify and separately evaluate the electron-electron, electron-phonon, and impurity scattering contributions to the quasiparticle lifetime. There is a clear correspondence between spectroscopic and transport data. A residual low-temperature spectral linewidth ($\Gamma_0 = 17$ meV) indicates that the three-dimensional nature of the electronic states cannot be neglected even in this quasi-two-dimensional material.

DOI: 10.1103/PhysRevB.64.115102 PACS number(s): 71.10.Ay, 71.55.Ak, 72.15.Lh

I. INTRODUCTION

Angle-resolved photoemission spectroscopy (ARPES) with high resolution is a momentum-selective probe of the low-energy quasiparticle (QP) excitations in solids.[1] This capability has been thoroughly exploited in recent investigations of complex materials, including the high-T_c cuprates,[2–4] the giant magnetoresistance manganites,[5] or certain classes of low-dimensional conductors,[6] where correlations shape ground states with peculiar properties. Crucial aspects of theoretical models of these systems have been addressed by ARPES, including the fundamental issue about the nature—Fermi liquid (FL) vs marginal FL or Luttinger liquid—of their *normal* states. In principle, the spectroscopic data may discriminate between the conflicting scenarios, because of the close correspondence between ARPES spectra and the properties of the quasiparticles, embodied in the single-particle spectral function $A(k,\omega)$.[7]

In real experiments, however, perturbing effects beyond an idealized description of ARPES, may affect the interpretation of the data. Therefore it is important to develop a solid experimental base and a clear understanding of the spectral properties of materials that can be classified as Fermi liquids based on their thermodynamic and transport properties, as a reference for the more complex systems. Such ARPES investigations of standard metals verified some of the theoretical predictions, but also revealed unexpected complexities.[8]

Due to the kinematics of the photoemission process, the simple hole spectral response is not experimentally accessible in three-dimensional solids[1,9] but it can be observed for two-dimensional (2D) surface states, or quantum well states.[10] Layered compounds like the transition metal (TM) dichalcogenides, which support quasi-2D states, are also well suited for QP line shape studies by ARPES.

Three main intrinsic phenomena influence the hole spectrum probed by ARPES: (i) electron-electron (e-e); (ii) electron-phonon (e-ph) interactions; and (iii) scattering by defects and impurities. Each of them limits the QP lifetime, and therefore contributes to the QP spectral linewidth. From the intrinsic linewidth, which can be estimated from high-resolution data, the various contributions may be identified, exploiting their specific energy and temperature dependences.

Near the Fermi surface the contribution of electronic correlations to the hole linewidth is small (a few meV in most circumstances). It exactly vanishes at the Fermi level, where the QP lifetime becomes infinite.[11] Nevertheless, this term has been identified in high-resolution ARPES spectra of $1T$-$TiTe_2$,[8] which could be described by an asymptotic FL model near the Fermi surface. Agreement between experiment and a more general FL expression was also claimed further away from E_F.[12]

Electron-phonon scattering is the predominant broadening factor for the low-energy excitations in highly perfect single crystals. Its spectral consequences have been studied by ARPES on surface states[13–19] and quantum well states,[20] revealing moderate to strong electron-phonon interactions.

Despite the vast literature on disorder in solids, little is known about the influence of disorder on the spectral properties of the quasiparticles. Preliminary studies indicate a correlation between the ARPES line shape of surface states and the presence of absorbates[17] or the surface morphology.[21]

We have studied by high-resolution ARPES pure and disordered specimens of the quasi-2D material $1T$-$TiTe_2$, which has been identified as a model Fermi liquid system in recent ARPES work.[8,22–25] $1T$-$TiTe_2$ exhibits normal metallic properties over a broad temperature range, a band structure well described by theory, and a simple Fermi surface. Moreover, atomically flat and ordered surfaces may be prepared easily by cleavage in ultrahigh vacuum. All these characteristics make it an almost ideal material for a spectroscopic study of quasiparticle properties. Previous ARPES work on $1T$-$TiTe_2$ has clarified the overall electronic structure of this com-

pound, and addressed the issue of electronic correlations. Here we present a comparative analysis of the various quasiparticle scattering mechanisms based on spectroscopic and resistivity data. In this investigation we take advantage of the unique possibility of creating controlled amounts of random point defects by electron irradiation.

We find that both the residual electrical resistivity $\rho(T=0)$ and the spectral linewidth scale with the defect density. The quasiparticle lifetime measured at the Fermi surface by ARPES is proportional to the relaxation time derived from transport experiments. From an analysis of the temperature dependence of the spectral linewidth we also obtain an estimate for the electron-phonon coupling parameter λ. The weak-coupling value $\lambda=0.22$ is consistent with the absence of superconductivity or charge-density-wave (CDW) instabilities. Our line shape analysis indicates a residual low-temperature linewidth which cannot be accounted for by the hole scattering processes, and which we attribute to the finite photoelectron lifetime. The observation of this broadening mechanism, which would be absent in a strictly 2D system, indicates the limits of a description of layered materials that neglects the 3D coupling between planes.

II. EXPERIMENT

Single-crystal specimens of $1T$-$TiTe_2$ were grown by the usual iodine vapor transport method. After an optimization of the growth parameters we obtained thick plaquettes with typical dimensions $4\times4\times0.2$ mm^3. Several samples chosen from a single batch were exposed to a 2.5 MeV electron beam at the Laboratoire de Solides Irradiés of the Ecole Polythechnique. During the irradiation the samples were immersed in liquid H_2. Previous experiments on layered chalcogenides have shown that electron irradiation creates random point defects in the metal planes by displacing the metal atoms from their equilibrium position.[26] The defect concentration is proportional to the integrated flux expressed by the electron fluence Φ_t (e cm^{-2}). The structural effects of growing disorder were monitored by Bragg diffraction, which showed a progressive increase of the width of the θ-2θ rocking curves, indicative of a reduced crystalline coherence length.

We measured the in-plane and out-of-plane dc resistivities in the 4–300 K temperature range by a standard four-point method. We performed ARPES experiments in Lausanne with a Scienta SES-300 hemispherical analyzer and a He lamp ($h\nu=21.2$ eV), and at the Swiss-French SU3 undulator beamline of the SuperAco storage ring (Orsay). The samples were mounted on a He flow cryostat, where the temperature could be varied between 300 K and 13 K, and cleaved *in situ* at the base pressure of 1×10^{-10} mbar. For the high-resolution data presented here, the overall energy resolution was 8 meV, as determined from the metallic edge of a polycrystalline Au film. The accuracy of the Fermi level position was ±0.5 meV. The acceptance angle was $\pm0.5°$ ($\Delta k=\pm0.04$ Å^{-1}) in the dispersive direction, and $\pm1°$ in the perpendicular direction.

III. STRUCTURAL AND ELECTRONIC PROPERTIES OF $1T$-$TiTe_2$

$1T$-$TiTe_2$ exhibits a layered structure, typical of TM dichalcogenides, where Ti atoms are confined in planes sandwiched between Te layers. Adjacent layers are separated by van der Waals gaps and interact weakly with each other. The crystal structure is $1T$-CdI_2 (space group D_{3d}^3) with lattice parameters $a=3.8$ Å and $c=6.5$ Å.[27] Each metal atom is surrounded by a distorted octahedron of anions with a trigonally symmetric projection in the plane. The Brillouin zone (BZ) has a threefold symmetry, with inequivalent ΓM and $\Gamma M'$ directions.

In a purely ionic picture the Te $5p$ bands would be full, and the Ti $3d$ bands completely empty. The Ti $3d$ states are split into t_{2g} and e_g manifolds, and the d_{z^2} states are further split off from the t_{2g} manifold as a consequence of the trigonal distortion. The partial overlap of these states with the Te $5p$ bands is responsible for the observed semimetallic behavior of $1T$-$TiTe_2$. The Ti d_{z^2} band forms electron pockets around the M and M' points, strongly stretched along the ΓM direction.[24]

The electronic properties of $1T$-$TiTe_2$ are rather anisotropic, and typical of a quasi-2D material. The electrical resistivity is metallic and, unlike in other 2D TM dichalcogenides, it does not suggest the occurrence of CDW transitions.[28] For our pristine samples, the room temperature in-plane resistivity was in the 100–120 $\mu\Omega$ cm range. The out-of-plane component was larger by a factor of 35–40, and the anisotropy was almost temperature independent.

IV. THE ARPES LINE SHAPE

An ideal ARPES experiment measures, apart from dipole transition matrix elements, the momentum-dependent single-particle spectral function $A(k,\omega)$:[7]

$$A(k,\omega)=\frac{1}{\pi}\frac{\mathrm{Im}\Sigma(k,\omega)}{[\omega-\varepsilon(k)-\mathrm{Re}\Sigma(k,\omega)]^2+[\mathrm{Im}\Sigma(k,\omega)]^2}. \tag{1}$$

$A(k,\omega)$ describes the removal of one particle (creation of one hole) in the many-body system. $\varepsilon(k)$ contains the band structure of the ideally noninteracting system, and all correlation effects are lumped into the self-energy $\Sigma(k,\omega)$. Σ is usually strongly energy dependent while the k dependence is weaker and often neglected. Σ has a twofold effect: it renormalizes the dispersion relation $\varepsilon(k)$, and it introduces a finite spectral linewidth $\Gamma=2\mathrm{Im}\Sigma$, which reflects the lifetime ($\tau=\hbar/\Gamma$) of the QP's in the interacting system.

All scattering mechanisms (electron-electron, electron-phonon, electron-impurities) contribute to Σ. In a first approximation the three terms are additive:

$$\Sigma=\Sigma_{e\text{-}e}+\Sigma_{e\text{-}ph}+\Sigma_{imp}. \tag{2}$$

Simple phase space considerations[7] show that the electron-electron self-energy $\Sigma_{e\text{-}e}$ must have the asymptotic form (for $\omega\rightarrow0$)

$$\Sigma_{e\text{-}e}(\omega)=\alpha\omega+i\beta[\omega^2+(\pi k_B T)^2]. \quad (3)$$

The temperature-dependent term is always very small and can be neglected with respect to the ω^2 and other T-dependent terms (see below). Further away from the Fermi surface more general expressions, satisfying the causality condition, have been proposed.[12] In the following we will be concerned with low-energy excitations, for which the simple asymptotic expansion (3) is appropriate.

Lifetime broadening due to electron-phonon scattering becomes rapidly predominant with increasing temperature. The imaginary part of the e-ph self-energy is given by[29]

$$\mathrm{Im}\Sigma_{e\text{-}ph}(T,\omega)=\pi\int_0^\infty d\nu\alpha^2F(\nu)[2n(\nu)+f(\nu+\omega) + f(\nu-\omega)]. \quad (4)$$

Here $n(\omega)$ and $f(\omega)$ are, respectively, the Bose-Einstein and the Fermi-Dirac (FD) distributions, and $\alpha^2F(\omega)$ is the Eliashberg coupling function. Within the Debye model, $\alpha^2F(\omega)=\lambda(\omega/\Omega_m)^2$, and electron-phonon scattering is fully described by the coupling parameter λ and the cutoff frequency Ω_m of the phonon spectrum. Equivalently, at sufficiently high temperature the scattering rate at the Fermi surface ($\omega=0$) may be expressed as[28]

$$\hbar/\tau=\mathrm{const}+\pi\lambda k_B T. \quad (5)$$

$\mathrm{Im}\Sigma_{e\text{-}ph}$ has a quadratic (in 2D) ω dependence for $\omega<\Omega_m$, and it is constant for $\omega>\Omega_m$. $\mathrm{Re}\Sigma_{e\text{-}ph}$, which renormalizes the band dispersion, is appreciably different from zero only between 0 and Ω_m. We have verified *a posteriori* (see below) that both λ and Ω_m are small in $1T$-$TiTe_2$. In this case the choice $\mathrm{Re}\Sigma_{e\text{-}ph}=0$ and $\mathrm{Im}\Sigma_{e\text{-}ph}=\mathrm{Im}\Sigma(0,T)$ is a sufficient first approximation. Notice that this approximation may not be valid in systems with stronger e-ph interactions.

Scattering on impurities and crystalline defects generates a linewidth proportional to the defect concentration d. In a mean-field approach[30] and neglecting any possible energy dependence for QP's near the Fermi surface,

$$\Sigma_{imp}=i\Delta_{imp}(d). \quad (6)$$

The analysis of the ARPES data must also take into account the fact that the spectrum is actually the convolution of the hole spectral function, represented by $A(k,\omega)$, and the photoelectron spectral function. Therefore, in general, the spectral linewidth also includes a term reflecting the finite photoelectron lifetime. As discussed below, this term vanishes in a two-dimensional system, and in this limit only the hole lifetime contributes to the QP width.[9]

V. RESULTS AND DISCUSSION

A. Band dispersion and the electron-electron interaction

Figure 1 illustrates ARPES results for the pristine sample, measured at $T=13$ K along the ΓM high-symmetry direction of the BZ, in a narrow region around the Fermi surface. The spectra of $1T$-$TiTe_2$ are remarkable among other 2D materials for the large contrast between the narrow and intense QP feature and the very weak background. Both the width and the intensity of the dispersing peak exhibit a strong angular dependence, consistent with the literature.[8,23–25] These variations reflect the dispersion of the Ti d_{z^2} band across the Fermi level, with a small negative Fermi velocity. The sharp FD function ($\Delta E\sim 5$ meV) is mainly responsible for the rapid reduction of the spectral linewidth as the peak disperses through E_F.

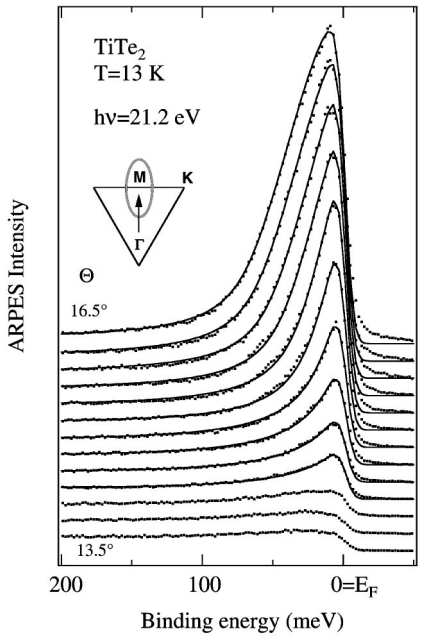

FIG. 1. High-resolution ARPES spectra of $1T$-$TiTe_2$ measured near the Fermi surface crossing along the high-symmetry ΓM direction ($\theta=0$ is normal emission). The lines are the results of Fermi liquid fits to the data with the parameters discussed in the text. The inset shows a portion of the Brillouin zone with the relevant ellipsoidal electron pocket.

We have analyzed the results of Fig. 1 within the FL scenario illustrated in Sec. IV. The parameters of the FL fit are the QP energy $\varepsilon(k)$ and the β coefficient of the asymptotic expansion [Eq. (3)] of the self-energy. All other intrinsic broadening mechanisms (impurities, finite temperature, photoelectron broadening) were modeled by a constant phenomenological term Γ_0 in $\mathrm{Im}\Sigma$. For each k value, the calculated spectral function was Gaussian broadened (full width at half maximum of 8 meV) to simulate the experimental energy resolution. Taking proper account of the finite angular resolution is less straightforward. The usual procedure, which consists in adding a constant phenomenological energy broadening to the spectra, is ill defined, especially when the band dispersion is anisotropic. Ideally, one should integrate the calculated spectrum over the acceptance angular window of the analyzer. We have implemented this procedure by modeling the shape of the constant energy contours, based on calculations and previous ARPES determinations of the Fermi surface[24] and on the local density approximation (LDA) estimates of the Fermi velocities.[8] The overall intensity of the spectra was left free to vary, thus allowing for matrix elements effects and experimental uncertainties in the normalization of the spectra.

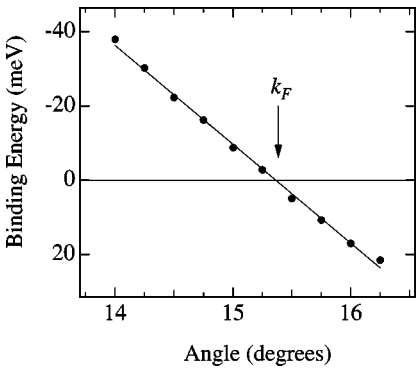

FIG. 2. Quasiparticle binding energy obtained from the FL fit of the high-resolution data of Fig. 1. The Fermi wave vector is determined from the Fermi level crossing of the interpolated linear dispersion.

Excellent fits to the measured spectra are obtained for $\Gamma_0 = 17$ meV, and for values of the parameter β varying between 0.5 eV^{-1} (16°) and 0.9 eV^{-1} (14.5°). The experimental spectra consistently exhibit some intensity above the FL fit in the leading edge near E_F. We attribute this small discrepancy to valence band photoelectrons generated by higher-energy satellites of the He I photon line, and to a slight deviation from a Gaussian instrumental response of the analyzer. The QP dispersion $\varepsilon(k)$ obtained from the fit (Fig. 2) is essentially linear in the small angular range considered (2°). The Fermi velocity $\hbar v_F = 0.73 \pm 0.1$ eV Å matches well the LDA value $v_{LDA} = 0.68$ eV Å,[8] and supports the choice made in the evaluation of the angular integration.

The determination of the Fermi level crossing of a metallic band from the ARPES data has become an increasingly important and debated issue. In the cuprates,[2–4] for instance, small differences in the shape and size of the Fermi surface may be essential to distinguish between competing theoretical models. Weak dispersing signals and, more importantly, the lack of a precise knowledge of the spectral line shape, limit the accuracy of the analysis, and have generated strong controversies.[31,32] Even for a simple metal, the determination of k_F is not unambiguous. Specific properties of the measured QP peak—its width, binding energy, intensity—or of the momentum distribution function $n(k)$ deduced from the ARPES data have been used as indicators of a Fermi level crossing. The various methods are not equivalent. For the well-studied case of $1T$-$TiTe_2$ there is a rather large spread in the estimates of k_F from the various approaches, ranging from 14.75° (0.53 $Å^{-1}$) (Ref. 8) to 16.7° (0.59 $Å^{-1}$).[25] From a linear interpolation of the data points of Fig. 2, we determine a Fermi level crossing at $k_F = 15.4° \pm 0.5°$. This yields $k_F = 0.55 \pm 0.02$ $Å^{-1}$, in good agreement with the recent detailed analysis of temperature-dependent data by Gweon.[23] The error bars include the estimated uncertainties of our analysis.

The tail on the low-kinetic energy side of the QP peak is a typical fingerprint of electronic correlations. The FL fit is quite sensitive to the intensity of this feature. The best fit value $\beta = 0.7 \pm 0.2$ eV^{-1} should be regarded as an upper limit because the overlapping contribution of the (weak) inelastic background may still lead to overestimating the intrinsic tail, especially when the peak intensity is small ($\theta < 15°$ in Fig. 1). Even then, it is considerably smaller than $\beta = 40$ eV^{-1} from Ref. 8, which is incompatible with a description of the electrical resistivity of $1T$-$TiTe_2$ based on the asymptotic form of the FL electron self-energy.[28] We stress the fact that the discrepancy is not in the quality of the FL fits, which is quite comparable, but rather in the interpretation of the broadening terms. While our fitting procedure allows for a constant contribution Γ_0, the analysis of Ref. 8 interprets the whole linewidth in terms of *e*-*e* scattering, thus neglecting other mechanisms which may be predominant near the Fermi surface.

More recently, Gweon *et al.*[23] reported that the incompatibility between the transport data and large β values may be removed in a more general FL scenario.[12] We notice, however, that smaller β values are supported by fundamental considerations which set a limit on the maximum strength of the *e*-*e* interaction in a metal. This is expressed by the condition $U < W$, where U is the on-site Coulomb repulsion and W is the total (occupied plus unoccupied) bandwidth. Larger values of U would lead to a Coulomb correlation gap, and a (Mott-Hubbard) insulating ground state. Within the Born approximation, the condition $U < W$ is equivalent to $\beta = \pi U^2/(4W^3) < \pi/(4W)$.[17] Replacing W by the LDA bandwidth (0.8 eV) of $1T$-$TiTe_2$,[8] we obtain $\beta < 1$ eV^{-1}, which agrees well with $\beta = 0.7$ from our line-shape analysis.

B. The temperature dependence of the quasiparticle lifetime

Scattering between electrons on the Fermi surface is forbidden, at $T = 0$, by Pauli's principle. In these conditions, if only electron-electron and electron-phonon scattering processes were active, the QP lifetime would be infinite. The QP's at the Fermi surface still acquire a finite lifetime, and a finite Lorentzian linewidth, through scattering by impurities and, at finite temperatures, by phonons. In this section we consider the temperature dependence of the QP lifetime, which reflects electron-phonon interactions, since impurity scattering is temperature independent, and the T-dependent term in $\Sigma_{e\text{-}e}$ [Eq. (3)] is always quite small.

Figure 3 shows ARPES data measured between 13 K and room temperature at the ΓM Fermi surface crossing of Fig. 1. As expected, the spectrum is sharpest at the lowest temperature. The peak appears at a finite binding energy, rather than at E_F, due to the combined effects of the FD function, and of the finite experimental resolution. With increasing temperature the progressive broadening of the FD function shifts spectral weight back toward E_F. At the same time, the peak intensity decreases, and the width increases due to increasing electron-phonon scattering.

The temperature-dependent spectral linewidth $\Gamma(T)$—the half width at half maximum (HWHM) of the underlying Lorentzian line shape—decreases almost linearly from room temperature down to 70 K, and then saturates at low temperature. This dependence is well reproduced by the electron-phonon self-energy [Eq. (4)] plus a constant term $\Gamma_0 = 17$ meV. The best agreement over the whole temperature range (dashed line in Fig. 4) is obtained for an *e*-ph coupling constant $\lambda = 0.22$ and a Debye cutoff frequency

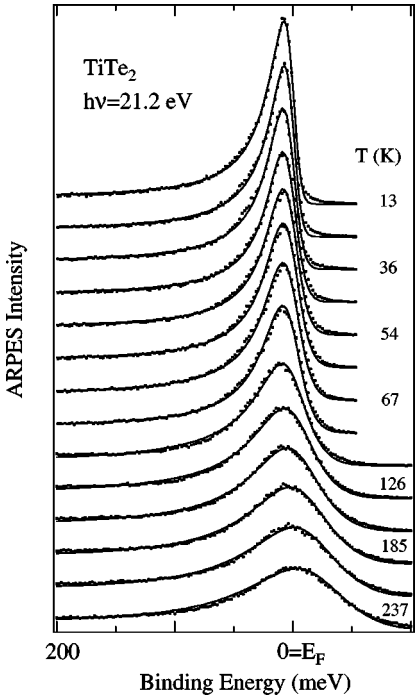

FIG. 3. ARPES spectra of $1T$-$TiTe_2$ measured at the Fermi surface at various temperatures. The lines are the result of a FL fit with a temperature-dependent self-energy describing electron-phonon scattering.

$\hbar\Omega_m = k_B\Theta_D = 20$ meV. The small λ is consistent with the absence of superconducting or CDW transitions in $1T$-$TiTe_2$ down to 1 K. On the other hand, neither the e-e nor the e-ph scattering mechanisms, which vanish at $T=0$, can account for the residual low-temperature linewidth. Therefore Γ_0 must reflect contributions from impurity scattering and from other extrinsic effects, as discussed in a later section.

The temperature evolution of the spectral function is illustrated in a direct way by Fig. 5. Following a procedure that is now common in high-T_c work, each spectrum was symmetrized around the Fermi energy to remove the FD cutoff: $I^*(\omega) = I(\omega) + I(-\omega)$. Under the assumption of

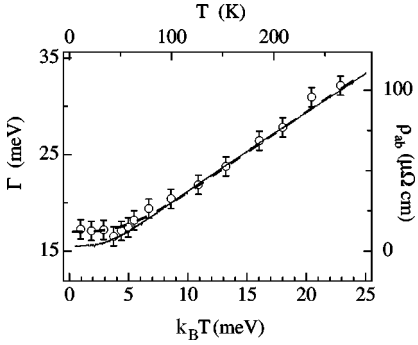

FIG. 4. Comparison of the temperature-dependent spectral linewidth Γ (HWHM) (open symbols) from Fig. 3, with the in-plane electrical resistivity ρ_{ab} (solid line). The dashed line illustrates the theoretical prediction for an electron-phonon coupling parameter $\lambda = 0.22$ plus a constant term $\Gamma_0 = 17$ meV. Notice the offset between the two vertical scales.

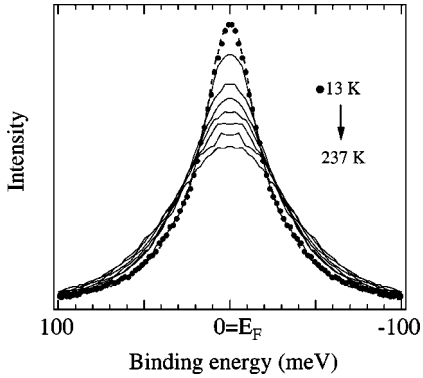

FIG. 5. Symmetrized curves $[I^*(\omega) = I_0(\omega) + I_0(-\omega)]$ obtained from the Fermi surface ARPES spectra of Fig. 3, showing the thermal broadening of the QP peak. The maxima of the curves are at the Fermi level at all temperatures. Notice the overlap of the 13 K (solid circles) and 54 K (dashed line) spectra.

electron-hole symmetry $[A(k_F,\omega) = A(k_F,-\omega)]$, which is certainly satisfied near the Fermi surface, $I^*(\omega)$ is then simply proportional to $A(k,\omega)$. Indeed, all the symmetrized curves exhibit maxima exactly at E_F, as expected for QP's at the Fermi surface. Having thus removed the FD cutoff, the temperature-dependent broadening and the saturation to an unvarying Lorentzian line shape below ~ 60 K are quite evident (notice the perfect overlap of the 13 K and 54 K curves).

It is instructive to compare the temperature dependence of the spectral properties of the QP's with a transport property like the electrical resistivity (Fig. 4). The in-plane resistivity $\rho_{ab}(T)$ exhibits a typical metallic behavior and, apart from the offset Γ_0, the same temperature dependence as the QP linewidth Γ. This is a strong indication that the transport relaxation time τ^* follows the spectroscopic lifetime τ. In other words, the transport properties of $1T$-$TiTe_2$ reflect the scattering of the quasiparticles. The good agreement between the two quantities is remarkable, and perhaps surprising for two reasons: (i) τ^* is an averaged value over the whole Fermi surface, while our QP analysis is limited to a specific point in k space; (ii) small-angle scattering events, which limit the QP lifetime, have a small effect on the electrical resistivity. A more accurate sampling of the Fermi surface will be necessary to clarify this observation.

One should note that the agreement between spectroscopic and transport lifetimes is not limited to a trivial rescaling of the two sets of data. Assuming a rigid-ion scattering potential, the resistivity and QP lifetime, are related by $\rho = (4\pi\Gamma/\Omega_p^2)$,[28,29,33] so that the ratio $\Delta\rho/\Delta\Gamma$ determines the plasma frequency Ω_p. From the data of Fig. 4 we obtain $\hbar\Omega_p = 1.1 \pm 0.1$ eV. We are not aware of experimental measurements of the plasma frequency in $1T$-$TiTe_2$, but our estimate is certainly in line with the plasma frequencies of other metallic TM dichalcogenides determined from optical data.[34]

C. The spectral consequences of disorder

In this section we compare spectroscopic and resistivity data for pristine $1T$-$TiTe_2$, with data from irradiated samples

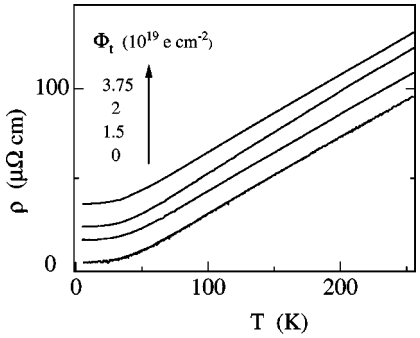

FIG. 6. Resistivity curves for pristine (bottom) and irradiated $1T$-$TiTe_2$ samples, with increasing amounts of disorder (expressed by the electron fluence Φ_t). Notice the identical slopes and the increasing residual resistivities.

with increasing amounts of disorder. From the tabulated cross sections and from previous irradiation experiments on other layered TM dichalcogenides[26] we estimate defect concentrations in the 10^{-3} to 10^{-2} dpa (displacements per atom) range in our irradiated samples [$\Phi_t = (1.5–3.75 \times 10^{19} e$ cm^{-2}]. The effect of disorder on the resistivity is clearly illustrated in Fig. 6. The slope of the $\rho(T)$ curves remains unchanged, indicating that neither the electron-phonon interaction nor the carrier concentration is affected by disorder. The curves are rigidly shifted upward in the more strongly irradiated samples. We conclude that the point defects created by fast electron irradiation introduce a residual resistivity ρ_0 proportional to the irradiation dose.

Disorder produces distinctive changes in the ARPES spectra. The spectra of the pristine sample and of an irradiated crystal ($\Phi_t = 3.75 \times 10^{19} e$ cm^{-2}), both measured at 13 K at the ΓM Fermi surface crossing, are compared in Fig. 7. The broader QP peak of the disordered sample reflects the shorter QP lifetime. Once again, the effect can be quantified by a FL analysis. The extracted Γ values, shown in Fig. 8, increase linearly from 17 meV in the pristine sample to 25 meV for the largest defect concentration. The similar dependence of Γ and ρ_0 on the amount of disorder confirms the proportionality between the transport relaxation time and the QP lifetime.[30]

Two semiquantitative considerations support this conclusion. The mean free path for QP scattering on the impurities

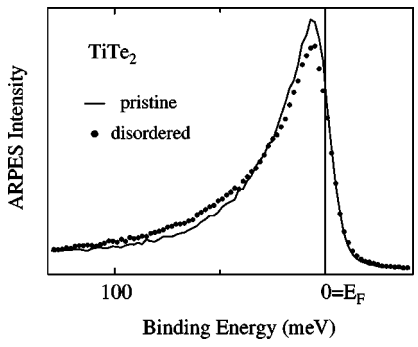

FIG. 7. High-resolution spectra at $k = k_F$ of a pristine and an irradiated ($\Phi_t = 3.75 \times 10^{19} e$ cm^{-2}) $1T$-$TiTe_2$ sample. The larger spectral width indicates a shorter lifetime in the disordered sample.

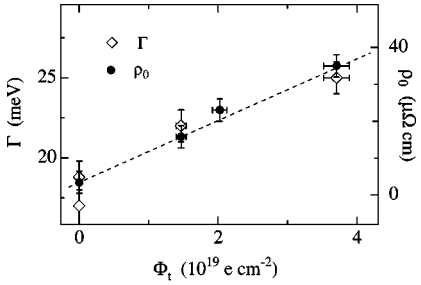

FIG. 8. Dependence on disorder (expressed by the electron fluence Φ_t) of the spectral linewidth Γ and of the residual resistivity ρ_0.

is $l = \tau v_F$. From the differences in the Γ values of Fig. 8, and the estimated v_F, we obtain $l \sim 100$ Å for the sample with the largest disorder.[35] The mean free path can also be expressed as $l = (a/d)$, where a is a lattice parameter and d is the density of scattering centers. For $l \sim 100$ Å and $a \sim 3$ Å we obtain $d \sim 3 \times 10^{-2}$ which is, within a factor of 2, the estimated density of irradiation defects for this sample. Furthermore, the ratio $(\Delta\rho/\Delta\Gamma)$, where the variations are now due to impurities, yields a plasma frequency $\Omega_p = 1.2 \pm 0.2$ eV, which is in excellent agreement with the value deduced from Fig. 4 in the different context of phonon scattering.

D. Finite photoelectron lifetime

The line shape analysis of the previous sections indicate the existence of a residual ($\Gamma_0 = 17$ meV) spectral linewidth in the pristine samples. At the measurement temperature ($T = 13$ K) both $\Sigma_{e\text{-}e}$ and $\Sigma_{e\text{-}ph}$ are very small at E_F. Still, their values at finite binding energies may affect the linewidth of a QP at the Fermi surface. The energy dependence of $\Sigma_{e\text{-}e}$ [Eq. (3)] is explicitly included in the FL fit. We have estimated the inaccuracy due to the simplifying assumption of a constant $\Sigma_{e\text{-}ph}$, and found it to be negligible with respect to Γ_0. Therefore we conclude that neither electron-electron nor electron-phonon scattering processes may explain the residual linewidth. The possible role of impurities must be assessed more carefully. The residual resistivity $\rho_0 = 2$ $\mu\Omega$ cm of the pristine sample is quite low, and more than one order of magnitude smaller than ρ_0 in the strongly disordered crystal, where the contribution of defects to the total Γ is only ~ 8 meV. We conclude that bulk defects in our pristine crystals can account for only a small part of the measured linewidth. We cannot exclude a larger concentration of surface defects, e.g., cleavage-induced defects, which could influence the measured spectra, given the large surface sensitivity of ARPES. This was observed for instance in high-resolution spectra of clean metal surfaces.[36] We notice, however, that various samples and cleaves consistently yielded similar Γ_0 values, suggesting that surface-related features do not represent the main contribution to the measured linewidth.

Another extrinsic broadening mechanism, typical of the photoemission process, may provide an alternative explanation. The ARPES spectrum measures the hole spectral func-

tion $A(k,\omega)$ only in the 2D limit. In a more general case the spectral linewidth has contributions both from the hole (Γ_h) and the electron (Γ_e) scattering rates. At normal emission, this is expressed by[9]

$$\Gamma = \frac{\Gamma_h + (v_{h\perp}/v_{e\perp})\Gamma_e}{1-(v_{h\perp}/v_{e\perp})}, \tag{7}$$

where $v_{h\perp}$ and $v_{e\perp}$ are the perpendicular (to the sample surface) components of the hole and photoelectron velocities. Therefore Γ reduces to Γ_h in the absence of perpendicular dispersion ($v_{h\perp}=0$), i.e., in a purely 2D system. Previous photoemission studies on noble metals[37] yielded $\Gamma_e = 0.07 \times h\nu$, where $h\nu$ is the photon energy. Using this value as a guideline, and free-electron final states for the photoelectron, the measured Γ yields $v_{h\perp}=0.12$ eV Å. By combining it with the in-plane Fermi velocity $\hbar v_F = 0.73$ eV Å, we obtain $(v_{h\|}/v_{h\perp})^2 = 37$, which is very close to the measured resistivity anisotropy, as expected from transport theory.[30] The small perpendicular Fermi velocity is consistent with the calculated dispersion of the Ti d_{z^2} band, and with the quasi-2D character of $1T$-$TiTe_2$. However, the line-shape analysis of the high-resolution data clearly demonstrates that this term cannot be neglected when the QP properties are evaluated, and that in fact it becomes predominant at low temperature and near the Fermi surface.

VI. CONCLUSIONS

We exploited high-resolution ARPES and samples with controlled amounts of bulk disorder to study the competing quasiparticle scattering mechanisms in the model FL system $1T$-$TiTe_2$. A Fermi liquid line-shape analysis of temperature-dependent ARPES spectra yields the fundamental parameters (β,λ) describing the electron-electron and electron-phonon interactions in this material. The spectral properties of the quasiparticles are consistent with the physical properties of $1T$-$TiTe_2$, namely, the absence of superconducting or charge-density-wave instabilities. We find that the quasiparticle lifetime derived from ARPES follows the transport relaxation time, namely, we observed the parallel linear growth of the spectroscopic and transport scattering rates in samples with increasing densities of random point defects.

The FL analysis of the data indicates a residual QP linewidth $\Gamma_0 \sim 17$ meV, which we attribute mainly to the contribution of the photoelectron lifetime. The three-dimensional character of the electronic states is clearly not negligible, and becomes the main source of spectral broadening near the Fermi surface and at low temperature. This observation invites a systematic evaluation of the influence of this term on the spectra of the complex and still poorly understood cuprates and layered CDW materials.

ACKNOWLEDGMENTS

We are indebted to Dr. D. Ariosa and I. Kezsmarki for their help with the x-ray diffraction and the transport measurements. We gratefully acknowledge correspondence with S. Shell. Work in Lausanne and at the Swiss-French beamline in Orsay was supported by the Swiss National Science Foundation.

*Also at LURE, Université de Paris-Sud, F-91405 Orsay, France.

[1] S. Hüfner, *Photoelectron Spectroscopy* (Springer-Verlag, Berlin, 1995).

[2] For entries in the huge literature on cuprates, see T. Valla, A.V. Fedorov, P.D. Johnson, B.O. Wells, S.L. Hulbert, Q. Li, G.D. Gu, and N. Kushizuka, Science **285**, 2110 (1999), and the following two references.

[3] A. Kaminski, J. Mesot, H. Fretwell, J.C. Campuzano, M.R. Norman, M. Randeria, H. Ding, T. Sato, T. Takahashi, T. Mochiku, and H. Hoechst, Phys. Rev. Lett. **84**, 1788 (2000).

[4] P.V. Bogdanov, A. Lanzara, S.A. Kellar, X.J. Zhou, E.D. Lu, W.J. Zheng, G. Gu, J.-I. Shimoyama, K. Kishio, H. Ikeda, R. Yoshizaki, Z. Hussain, and Z.X. Shen, Phys. Rev. Lett. **85**, 2581 (2000)

[5] D.S. Dessau, T. Saitoh, C.-H. Park, Z.-X. Shen, P. Villella, N. Hamada, Y. Moritomo, and Y. Tokura, Phys. Rev. Lett. **81**, 192 (1998).

[6] For a recent review, see M. Grioni and J. Voit, in *Electron Spectroscopies Applied to Low-Dimensional Materials*, edited by H. P. Hughes and H. I. Starnberg (Kluwer, Dordrecht, 2000), p. 209.

[7] L. Hedin and S. Lundqvist, in *Solid State Physics*, edited by F. Seitz, D. Turnbull, and H. Ehrenreich (1969), Vol. 23, p. 1.

[8] R. Claessen, R.O. Anderson, J.W. Allen, C.G. Olson, C. Janowitz, W.P. Ellis, S. Harm, M. Kalning, R. Manzke, and M. Skibowski, Phys. Rev. Lett. **69**, 808 (1992); R. Claessen, R.O. Anderson, G.-H. Gweon, J.W. Allen, C.G. Olson, C. Janowitz, W.P. Ellis, Z.-X. Shen, M. Skibowski, K. Friemelt, E. Bucher, S. Hüfner, and V. Eyert, Phys. Rev. B **54**, 2453 (1996); R. Claessen, Th. Straub, P. Steiner, S. Hüfner, V. Eyert, R.O. Anderson, J.W. Allen, C. Janowitz, and C.G. Olson, Physica B **230-232**, 294 (1997).

[9] N.V. Smith, P. Thiry, and Y. Petroff, Phys. Rev. B **47**, 15 476 (1993).

[10] J.J. Paggel, T. Miller, and T.-C. Chiang, Phys. Rev. Lett. **81**, 5632 (1998); Science **283**, 1709 (1999).

[11] P. Nozières, *Interacting Fermi Systems* (W.A. Benjamin Inc., New York, 1964).

[12] J.W. Allen, J.-H. Gweon, R. Claessen, and K. Matho, J. Phys. Chem. Solids **56**, 1849 (1995).

[13] B.A. McDougall, T. Balasubramanian, and E. Jensen, Phys. Rev. B **51**, 13 891 (1995).

[14] T. Balasubramanian, E. Jensen, X.L. Wu, and S.L. Hulbert, Phys. Rev. B **57**, R6866 (1998); S. LaShell, E. Jensen, and T. Balasubramanian, *ibid.* **61**, 2371 (2000).

[15] M. Hengsberger, D. Purdie, P. Segovia, M. Garnier, and Y. Baer, Phys. Rev. Lett. **83**, 592 (1999); M. Hengsberger, R. Frésard, D. Purdie, P. Segovia, and Y. Baer, Phys. Rev. B **60**, 10 796 (1999).

[16] Ph. Hofmann, Y.Q. Cai, Ch. Grütter, and J.H. Bilgram, Phys. Rev. Lett. **81**, 1670 (1998).

[17] T. Valla, A.V. Fedorov, P.D. Johnson, and S.L. Hulber, Phys. Rev. Lett. **83**, 2085 (1999).

[18] E. Rotenberg, J. Schaefer, and S.D. Kevan, Phys. Rev. Lett. **84**, 2925 (2000).
[19] G. Nicolay, F. Reinert, S. Schmidt, D. Ehm, P. Steiner, and S. Hüfner, Phys. Rev. B **62**, 1631 (2000).
[20] J.J. Paggel, T. Miller, and T.-C. Chiang, Phys. Rev. Lett. **83**, 1415 (1999)
[21] F. Theilmann, R. Matzdorf, and A. Goldmann, Surf. Sci. **420**, 33 (1999).
[22] D.K.G. de Boer, C.F. van Bruggen, G.W. Bus, R. Coehoorn, C. Haas, G.A. Sawatzky, H.W. Myron, D. Norman, and H. Padmore, Phys. Rev. B **29**, 6797 (1984).
[23] G.-H. Gweon, Ph.D. thesis, University of Michigan (1999).
[24] S. Hüfner, R. Claessen, F. Reinert, Th. Straub, V.N. Strocov, and P. Steiner, J. Electron Spectrosc. Relat. Phenom. **100**, 191 (1999).
[25] L. Kipp, K. Rossnagel, C. Solterbeck, T. Strasser, W. Schattke, and M. Skibowski, Phys. Rev. Lett. **83**, 5551 (1999).
[26] H. Mutka, L. Zuppiroli, P. Molinié, and J.C. Bourgouin, Phys. Rev. B **23**, 5030 (1981).
[27] Y. Arnaud and M. Chevreton, J. Solid State Chem. **39**, 230 (1981).
[28] P.B. Allen and N. Chetty, Phys. Rev. B **50**, 14 855 (1994).
[29] G. Grimvall, *The Electron-Phonon Interactions in Metals* (North-Holland, New York, 1981).
[30] J. M. Ziman, *Models of Disorder* (Cambridge University Press, Cambridge, 1979).
[31] N.L. Saini, J. Avila, A. Bianconi, A. Lanzara, M.C. Asensio, S. Tajima, G.D. Gu, and N. Koshizuka, Phys. Rev. Lett. **79**, 3467 (1997).
[32] Y.-D. Chuang, A.D. Gromko, D.S. Dessau, Y. Aiura, Y. Yamaguchi, K. Oka, A.J. Arko, J. Joyce, H. Eisaki, S.I. Uchida, K. Nakamura, and Yoichi Ando, Phys. Rev. Lett. **83**, 3717 (1999).
[33] J. M. Ziman, *Electrons and Phonons* (Oxford University Press, Oxford, 1972).
[34] L. Vescoli, L. Degiorgi, H. Berger, and L. Forro, Phys. Rev. Lett. **81**, 453 (1998).
[35] This number represents the actual mean free path in the disordered sample if impurity scattering is much weaker and the mean free path much longer in the pristine material. This assumption is consistent with the very small value of the residual resistivity.
[36] D. Purdie, M. Hengsberger, M. Garnier, and Y. Baer, Surf. Sci. **407**, L671 (1998).
[37] A. Goldman and W. Altmann, Solid State Commun. **79**, 511 (1991).